In vitro digestion of Pickering emulsions stabilized by soft whey protein microgel particles: influence of thermal treatment

Received 00th January 20xx,
Accepted 00th January 20xx

DOI: 10.1039/x0xx00000x

www.rsc.org/

Anwesha Sarkar[a*], Brent Murray[a], Melvin Holmes[a], Rammile Ettelaie [a], Azad Abdalla [a], Xinyi Yang [a]

Emulsions stabilized by soft whey protein microgel particles have gained research interest due to their combined advantages of biocompatibility and high degree of resistance to coalescence. We designed Pickering oil-in-water emulsions using whey protein microgels using a facile route of heat-set gel formation followed by mechanical shear and studied the influence of heat treatment on emulsions stabilized by these particles. The aim of this study was to compare the barrier properties of the microgel particles and heat-treated fused microgel particles at the oil-water interface in delaying the digestion of the emulsified lipids using an *in vitro* digestion model. A combination of transmission electron microscopy and surface coverage measurements revealed increased coverage of heat-treated microgel particles at the interface. The heat-induced microgel particle aggregation and, therefore, a fused network at the oil-water interface, was more beneficial to delay the rate of digestion in presence of pure lipase and bile salts as compared to that of intact whey protein microgel particles, as shown by measurements of zeta potential and free fatty acid release, plus theoretical calculations. However, simulated gastric digestion with pepsin impacted significantly on such barrier effects, due to the proteolysis of the particle network at the interface irrespective of the heat treatment, as visualized using sodium dodecyl sulfate polyacryl amide gel electrophoresis measurements.

1. Introduction

Emulsifiers play an important role in stabilizing the oil droplets by adsorbing at the oil-water interface. Besides conventional surfactants, such as mono or di-acylglycerols, proteins, etc., emulsions can also be stabilized by solid particles via the Pickering stabilization mechanism. Unlike surfactants, spherical rigid or soft solid particles can stabilize the dispersed phase based on their partial wettability by both phases, which is driven by the contact angle and surface tension at the interface. For instance, if the contact angle is smaller than 90°, particles are more wetted by the continuous phase in an O/W emulsion rather than the oil phase. Although the stabilization of colloids using particles at the interface was proposed a century ago by Ramsden [1] and proven four years later experimentally by Pickering [2], there has been a renewed upsurge of research interest, illustrated by the growing number of reviews in the last few years [3-10]. This is largely due to the demand for highly stable emulsions and the growing requirements for biocompatible surfactant-free 'clean-label' emulsifiers that are immediately suitable for use in food, pharmaceutical, cosmetics, agrochemicals and other allied soft matter applications. Under partial wetting conditions, the solid particles adsorbed at the oil-water interface are almost irreversibly adsorbed, thus providing high stability against coalescence as opposed to typical molecular surfactants. The free energy (E) required for particle desorption from the interface can be expressed using Equation (1) [9, 11]:

$$E = \gamma\pi r^2 (1 - |\cos\theta|)^2 \qquad (1)$$

where, γ is the oil-water surface tension, r is the radius of the particle and θ is the contact angle. Hence, even for nanometer sized particles (radius = 10 nm), the adsorption energy can be several tens of thousands of thermal energy (k_BT) at 298 K and the desorption energy is actually shown to be higher due to the energy involved in dissipation during the dislodging of the particles from the interface [12].

Pickering emulsions offer the opportunity for colloid scientists to address key questions concerning physiological processes that can be influenced by soft matter structuring. In particular, since lipid digestion is an interfacial process, largely controlled by the binding of lipase-colipase complex onto the surface of emulsified droplets, it seems possible to alter the kinetics and degree of lipid digestion by modification of the interfacial structures or controlling the transport of lipase [13-15], and in turn to potentially control satiety. However, in most surfactant- and protein-stabilized emulsions, the adsorbed layers are displaced by biosurfactants, in particular bile salts [16-20]. Thus, the interfacial structure of the initial emulsion is not necessarily retained in the physiological regime, to allow easy adsorption of the lipase-colipase complex to the bile adsorbed surface and thus enable lipolysis and release of fatty acids. Simplistically, one might expect lipid digestion to be controlled by strengthening the interfacial network that resists displacement by bile salts. Therefore, particle-stabilized interfaces offer a promising template for controlling displacement by bile and therefore lipid digestion, with the first evidence being reported on chitin nanocrystals [21]. If proven, Pickering emulsions could be used to address site-dependent controlled release of nutrients, drugs or bioactive moieties in food, pharmaceutical and personal care applications.

Although a great many studies have been conducted on Pickering emulsions using traditional inorganic or synthetic particles, there is a relative paucity of literature on food-compatible particulate materials from natural edible sources, examples, include cellulose nanocrystals [22], chitin nanocrystals [23], modified starch [24], soy protein nanoparticles [25], flavonoid particles [26], micellar casein coated nanoemulsion droplets [27] and whey protein microgels [28, 29]. Soft solid particles such as whey protein microgels can be a particularly effective system to resist displacement by bile salts

[a] *Food Colloids and Processing Group, School of Food Science and Nutrition, University of Leeds, LS2 9JT, United Kingdom.*
** E-mail: A.Sarkar@leeds.ac.uk*

because soft solid particles deform during adsorption increasing the adsorption energies by orders of magnitude relative to rigid particles [30].

Whey protein acceptability and biocompatibility has ensured its safe and widespread use in current food applications. In addition, the versatility of using intact whey protein microgel particles may offer favourable properties due to their heat sensitivity. Apart from the formation of particle layers, during heat treatment some ordering mechanisms involving hydrophobic, electrostatic and covalent crosslinking via disulphide bridges between whey protein microgel particles can be anticipated [31]. Such heat-induced aggregation of the microgel particles would mean that rather than forming a simple monolayer which is densely packed, a network of aggregated or fused particles were adsorbed, held together by attractive inter-particle forces arising from those bonds.

Our hypothesis is that fused (heat-treated)-microgel stabilized interfaces should be able to protect the lipids against the action of lipase more significantly as compared to the non-heat treated intact whey protein microgel particles and thus contribute to delaying lipid digestion. Particle size characterization, zeta-potential measurements, confocal and electron microscopic observations, surface coverage and *in vitro* gastrointestinal digestion with pH-stat based free fatty acid release have been carried out. Since protein-based microgels are used, the influence of pepsin on the proteolysis of microgel particles and heat-treated microgel particles adsorbed at oil-water interface during gastric digestion was also studied using SDS-PAGE (sodium dodecyl sulphate polyacryl amide gel electrophoresis) to understand the fate of those particles post gastric transit.

A key question to be answered was whether such pepsin-driven proteolysis (if any) of the interfacial microgel particles (with and without heat treatment) in the gastric regime affected the kinetics of release of free fatty acids from the emulsified lipid droplets by the action of lipase in presence bile salts. Hence, firstly the behaviour during *in vitro* gastrointestinal digestion of both heat-treated and non-heat-treated whey protein microgel-stabilized emulsions was investigated in presence of bile and pancreatin (containing protease, lipase and amylase) post gastric digestion by pepsin. And, another model experiment was conducted in which only intestinal digestion was followed in presence of "pure lipase" and bile salts in order to understand the mechanism by which particles retard or restrict the access of pure lipase during intestinal digestion without pre-gastric digestion and without influence of any pancreatic proteases, supported by theoretical considerations. To our knowledge, this is the first study on digestive behaviour and restriction of bile salts displacement by intact or fused protein based on soft microgel particles at oil-water interfaces, which might serve as a route for designing novel encapsulation systems.

2. Experimental

3.1 Materials

Whey protein isolate (WPI) with ≥ 90% protein content was purchased from Fonterra Co-operative Group Limited, Auckland, New Zealand. Sunflower oil was purchased from a local supermarket. Porcine pepsin (P7000, actual activity: 526 U/mg), porcine pancreatin (P7585, 8 × USP), porcine bile extract B8631 (total bile salt content 49 wt%; with 10-15% glycodeoxycholic acid, 3-9% taurodeoxycholic acid, 0.5-7% deoxycholic acid; phospholipids 5 wt%) were purchased from Sigma-Aldrich Company Ltd., Dorset, UK. Pure lipase (activity 12,000 units/g solid) extracted from porcine pancreas was purchased from MP Biomedicals, Cambridge, UK. All other chemicals used were of analytical grade unless otherwise specified. Milli-Q water (water purified by treatment with a Milli-Q apparatus, Millipore Corp., Bedford, MA, USA) was used for all experiments.

3.2 Methods

2.2.1 Preparation of whey protein microgel

Whey protein microgel (WPM) particles were prepared by an adapted processing route based on the design principles of Schmitt *et al.* [32], via the disulphide crosslinking of WPI. Whey protein solution (10 wt%) was prepared by dissolving WPI powder in 20 mM phosphate buffer at pH 7.0 for 2 hours before storage at 4°C overnight to ensure complete solubilisation. The WPI solutions were heated at 90 °C for 30 minutes and cooled at room temperature for 30 minutes followed by storage at 4 °C overnight to form WPI gels. The gels were mixed with 20 mM phosphate buffer (1:1 w/w) at pH 7.0 and were pre-homogenized by a blender (HB711M, Kenwood, UK) for 10 minutes before homogenizing using two passes through a two-stage valve homogenizer (Panda Plus 2000, GEA Niro Soavi Homogeneizador Parma, Italy) operating at first / second stage pressures of 250 / 50 bar, respectively. The resulting 5 wt% whey protein microgel particle (WPM) was diluted to 1 wt% before emulsion preparation. The WPM particles generated using this approach was replicated three times in pilot scale.

2.2.2 WPM-stabilized pickering emulsion preparation and thermal treatment

Pickering emulsions were prepared by mixing 20.0 wt% sunflower oil and 80.0 wt% aqueous dispersions, containing 1 wt% WPM particles in the final emulsion. The mixture of sunflower oil and WPM solution was sheared using a conventional rotor-stator type mixer (L5M-A, Silverson machines, UK) at 5000 rpm for 5 minutes. The pre-emulsions were then homogenized by two passes through the Panda Plus 2000 homogenizer operating as above.

For preparation of the heat treated WPM-stabilized emulsion (HT-WPM), the emulsions stabilized by WPM were heat treated in a water bath at 90 °C for 30 min. Both the WPM and HT-WPM emulsion samples were prepared in triplicates.

2.2.3 Transmission electron microscopy (TEM)

Transmission electron microscopy (TEM) was employed to observe the microstructure of WPM particles, WPM-stabilized emulsions and HT-WPM stabilized emulsions. 10 µl of samples were fixed with 2.5% (v/v) glutaraldehyde and post fixed in 0.1% (w/v) osmium tetroxide [33]. The samples were then carefully exposed to serial dehydration in ethanol (20-100%)

before being embedded in araldite. Ultra-thin sections (silver-gold 80-100 nm) were deposited on 3.05 mm grids and stained with 8% (v/v) uranyl acetate and lead citrate. The sections were cut on an "Ultra-cut" microtome. Images were recorded using a CM10 TEM microscope (Philips, Surrey, UK).

2.2.4 Determination of surface coverage by microgel particles

To determine the amount of WPM at the interface of emulsion droplets, both WPM and HT WPM-stabilized emulsions were centrifuged for 20 min at 45,000 g and 20 °C (Sorvall RC5C, DuPont Co., Wilmington, DE, USA). The subnatants were carefully removed using a syringe and then filtered sequentially through 0.45 and 0.22 µm filters (Millipore Corp., Bedford, MA, USA). The filtrates were detected by a UV-Vis Spectrophotometer at an absorption wavelength of 595 nm using DC protein assay kit (Bio-Rad Laboratories, Hercules, CA). The surface coverage (mg/m^2) in case of both the emulsion droplets was calculated from the mean diameter of the oil droplets and the difference between the amount of WPM added to the emulsion and that measured in the subnatant [34]. The adsorption efficiency was calculated as the ratio of amount of protein adsorbed at the interface to the total amount of protein used for initial emulsion preparation.

2.2.5 *In vitro* digestion of emulsions and fatty acid release

Emulsions (both WPM and HT WPM-stabilised) were digested by subjecting them to sequential incubation in simulated gastric fluid (SGF) mimicking fasted conditions of stomach and then simulated intestinal fluid (SIF) using slightly adapted digestion protocol of Minkeus et al.[35], in a stirred double jacketed reaction vessel maintained at 37 °C. Briefly, 10 mL of each emulsion (20 wt% fat) was incubated for 2 hours with 10 mL of simulated gastric fluid (SGF), which consisted of, 0.257 g L^{-1} KCl, 0.061 g L^{-1} KH_2PO_4, 1.05 g L^{-1} $NaHCO_3$, 1.38 g L^{-1} NaCl, 0.122 g L^{-1} $MgCl_2(H_2O)_6$, 0.024 g L^{-1} $(NH_4)_2CO_3$ and 3.2 g L^{-1} pepsin at pH 2.0 at 37 °C. As a control, WPM solution was also subjected to SGF treatment.

After 2 hours of incubation in SGF, the pH of the emulsion-SGF was adjusted to pH 6.8 with dilute 1M NaOH and mixed 1:1 w/w with SIF. The SIF contained 0.253 g L^{-1} KCl, 0.054 g L^{-1} KH_2PO_4, 3.57 g L^{-1} $NaHCO_3$, 1.12 g L^{-1} NaCl, 0.335 g L^{-1} $MgCl_2(H_2O)_6$, 0.44 g L^{-1} $CaCl_2.2H_2O$, 0.23 g L^{-1} bile salts and 125 mg mL^{-1} pancreatin (2800 U, 63 U/mL). The temperature and pH were adjusted at 37 °C and pH 6.8, respectively. The intestinal digestion was carried out over 3 hours whilst maintaining the pH at 6.8 by addition of 0.05 M NaOH using a pH-Stat (TIM 854, Radiometer). In a separate experiment, pure lipase (12000 U, 260 U/mL) in SIF buffer was added to observe the intestinal digestion effect in absence of any pre-gastric proteolytic step. The volume of 0.05 M NaOH added to the samples was used to calculate the concentration of free fatty acids (FFA) generated in the reaction vessel during digestion of the emulsified lipids. The percentage of FFA released was calculated from the number of moles of NaOH required to neutralize the FFA that could be produced from the triacylglycerols if they were all digested (assuming the generation of 2 FFAs per triacylglycerol molecule by the action of lipase action) using Equation 2 [36]:

$$\%\mathrm{FFA} = 100 \times \left(\frac{\mathrm{V_{NaOH}} \times \mathrm{M_{NaOH}} \times \mathrm{M_{WLipid}}}{2 \times \mathrm{W_{Lipid}}} \right) \quad (2)$$

where, V_{NaOH} is the volume (mL) of sodium hydroxide, M_{NaOH} is the molarity of the sodium hydroxide solution used (0.05 M), M_{WLipid} is the average molecular weight of sunflower oil (0.880 kg mol^{-1}) and W_{Lipid} is weight of lipid initially present in the reaction vessel (0.4 g). In many if not most emulsions, the fatty acid released (Φ) gradually increases with time t , potentially attaining the total release (Φ_{max}).

To derive an expression for the variation of (Φ) with time t, we first note that for Pickering type emulsions the decrease in the volume of the droplets ceases very early on in the process. This is in marked contrast to cases involving surfactant or protein stabilised emulsions [29]. Indeed one of the major advantage of Pickering emulsions is their robustness against dissolution and shrinkage mechanisms such as Ostwald ripening [9]. We denote the fraction of converted lipid in the oil/water emulsion at time *t* by $\alpha(t)$. Then the mole fraction converted in a droplet of diameter d_0 is given by

$$\alpha(\mathrm{t}) \frac{\pi \mathrm{d}_0^3}{6} \frac{\rho_0}{\mathrm{M_w}} \quad (3)$$

where ρ_0 and M_w are the density and molar weight of lipid, respectively. Since the lipase only resides at the interface, one can assume that the rate of conversion is proportional to the surface area of the droplet[29] and furthermore that it is dependent upon the unconverted lipid proportion (1-α (*t*)), as well as the coverage of surface active lipase on the interface. Let us take the droplet surface coverage by bile salt/lipase at time *t* as $\Gamma_{en}(t)$ and assume that this coverage may achieve a maximum of Γ_{en}^{Max}, where the lipid conversion rate constant also achieves its maximum value, represented here by *k* (s^{-1} m^{-2}) defined as per unit area of the droplet surface. Typically, the lipase-colipase complex has a molecular radius of gyration of 25Å [45] thus a coverage of 2.66 x 10^{-7} moles m^{-2} is estimated for Γ_{en}^{Max}. Accordingly, sub-maximal conversion rate constant (per unit area) when the coverage of lipase/bile salt has not reached its plateau value is given by

$$\frac{\Gamma_{\mathrm{en}}(\mathrm{t})}{\Gamma_{\mathrm{en}}^{\mathrm{Max}}} \mathrm{k} \quad (4)$$

Then, at time t, the rate of conversion within the droplet is given as,

$$\frac{\Gamma_{\mathrm{en}}(\mathrm{t})}{\Gamma_{\mathrm{en}}^{\mathrm{Max}}} \mathrm{k} \pi \mathrm{d}_0^2 (1-\alpha) \quad (5)$$

where, πd_0^2 is the surface area of a droplet. In forming Eq 5 we assume that the composition of the droplet remains homogenous throughout. This would be the case if the diffusion of unconverted/converted oil between the surface and interior of the

droplet is rapid. We have proceeded to model the digestion of HT WPM particles at interface by assuming that the arrival of lipase is slow enough, thus having an impact on the rate of conversion and the process of adsorption to the surface is diffusion limited. We note that for short initial time t it is reasonable to suppose that all the bile/lipase arriving at the droplet surface will be adsorbed. This would not be the case at later times when saturation at the surface occurs. Thus for short times the coverage of lipase on surface increases linearly with time:

$$\Gamma_{en}(t) \cong \lambda n_{en} t \tag{6}$$

This is true whether the process is barrier limited or diffusion limited. So for example, in the diffusion limited case, the constant λ would be as $\lambda = 2D_{en}/d_0$, whereas for barrier limited case it will depend on the nature, structure and thickness of the adsorbed layer. Here, $2D_{en}/d_0$ is the diffusive flux of the lipase/bile salt incident on the droplet surface, with D_{en} denoting the diffusion coefficient of the enzyme (typically 10^{-9} – 10^{-10} m^2 s^{-1}) in the continuous aqueous phase and n_{en} its molar concentration in the bulk solution. For the barrier limited adsorption the constant term multiplying time in Eq 6 would obviously be different and determined by other factors (*e.g.* thickness and nature of a barrier layer). If sufficient enzyme is present in the aqueous phase so that even at the point of saturation of the surface of all droplets the concentration of enzyme remains approximately constant, then equating the rate of change of Eq 3 with Eq 5 and using equations 4 and 6, we arrive at the following equation for $\alpha(t)$:

$$\left(\frac{\pi d_0^3 \rho_0}{6M_w}\right)\frac{d\alpha}{dt} = k\frac{2D_{en}}{d_0\Gamma_{en}^{Max}} n_{en}\pi d_0^2(1-\alpha)t \tag{7}$$

Solving the above with the initial condition that $\alpha = 0$ at $t = 0$, we obtain

$$\alpha(t) = \frac{\phi(t)}{\phi_{max}} = \left(1 - \exp\left(\frac{-6kM_w D_{en} n_{en} t^2}{\rho d_0^2 \Gamma_{en}^{Max}}\right)\right) \tag{8}$$

valid for short times following the commencement of the experiment. On the other hand, if we consider the behaviour of the system at long times t, where the surface coverage of bile salt has reached its plateau value, then $\Gamma_{en}(t) \cong \Gamma_{en}^{Max}$

$$\alpha(t) = \frac{\phi(t)}{\phi_{max}} = \left(1 - \exp\left(\frac{-6kM_w t}{d_0\rho_0}\right)\right) \tag{9}$$

Obviously it is expected that this would be the case almost from the onset if the diffusion of enzyme onto the surface of droplets was a rapid process and that there were no barriers to limit the adsorption. For such cases then, one may take equation 9 as providing the time evolution of α throughout the entire conversion period.

Here, equation 8 describes the situation relevant to that of WPM Pickering stabilised droplet. For such a system, the enzyme is rapidly adsorbed to the surface and saturation is achieved rather quickly. This is because the gap between the Pickering particles is large enough for enzyme to move to the surface of droplets unhindered, a point that we shall briefly discuss later. In contrast, for the case of the heat treated microgel emulsion, particles fuse together and therefore there is the possibility of formation of a barrier limiting the rapid adsorption of the lipase. The expressions derived above from first-order kinetics assume that as the conversion proceeds, the rate of reaction reduces accordingly. Also, we ignore interfacial enzymatic mechanisms and utilise the assumption that the rate of lipid digestion is purely dependent upon the initial mean diameter d_0 of the emulsion droplets and that the number of droplets remains constant during digestion.

Consequently, the moles *k* of FFAs produced during lipolysis are per unit time and unit surface area (measured in mol s^{-1} m^{-2}) can be obtained from numerical fits of equations 8 and 9 to the experimental data. Here, ρ_0 for the density of oil is 910 kg m^{-3}. The lipolysis half time ($t_{1/2}$) (minutes) is the time required to achieve half lipid digestion and can be obtained from equations 8 and 9, respectively. The values thus calculated were used to compare the digestion profiles of the emulsion samples before and after heat treatment,

$$t_{1/2} = \sqrt{\ln(2)\frac{d_0^2 \rho_0 \Gamma_{en}^{Max}}{6kD_{en} n_{en} M_w}} \tag{10}$$

$$t_{1/2} = \ln(2)\frac{d_0\rho_0}{6kM_w} \tag{11}$$

for equations (8) and (9), respectively. We used Solver supplement of MS Excel (Microsoft Corporation) to solve for values of Φ_{max} and *k* which provided the best mathematical fit of our equations above to our experimental results.

2.2.6 Particle size and ζ-potential measurements

The mean hydrodynamic diameter of the WPM particles was measured by dynamic light scattering at 25 °C via a Zetasizer Nano ZS (Malvern Instruments Ltd., Malvern, Worcestershire, UK) equipped with a 4 mW helium/neon laser at a wavelength output of 633 nm. Droplet sizing was performed at 10 s intervals in a particle-sizing cell using backscattering configuration at a detection angle of 173 °C. The intensity of light scattered from the droplets was used to calculate the mean hydrodynamic diameter (Z-average), based on the Stokes-Einstein equation, assuming the emulsion droplets to be spherical.

Particle size distributions of WPM particles, WPM- and HT WPM-stabilized emulsions before and after gastric digestion (1, 5, 10, 30, 60, 90, 120 minutes and after intestinal digestion (30, 60, 90, 120, 150 and 180 minutes) were measured immediately by Malvern MasterSizer 3000 (Malvern Instruments Ltd., Malvern, Worcestershire, UK). For the parent and digested emulsion samples, the relative refractive index,

i.e., the ratio of sunflower oil (1.456) to that of dispersion medium (1.33) was 1.095 [34]. The absorbance of the emulsion droplets was set to 0.001. Droplet size measurements are reported as average Sauter mean diameter (d_{32}) and volume mean diameter (d_{43}) from the particle size distributions, using Equation 12:

$$d_{ab} = \frac{n_i d_i^a}{n_i d_i^b} \quad (12)$$

where, n_i is the number of particles with diameter d_i. Mean particle diameters were calculated as the average of five measurements.

The ζ-potential values of WPM- and HT-WPM-stabilized emulsions after digestion at different times were determined using a laser Doppler velocimetry and phase analysis light scattering (M3-PALS) technique and Zetasizer Nano ZS (Malvern Instruments Ltd., Malvern, Worcestershire, UK). The samples were diluted to 0.01 wt% droplet concentrations, placed in the electrophoretic mobility cell, and analysed at an angle of 173°. The effective electric field, E, applied in the measurement cell was between 50 and 150 V depending on the ionic strength of the samples. The electrophoretic mobility, μ, was calculated assuming spherical particles at 20 °C according using Equation 13:

$$\mu = \frac{v}{E} \quad (13)$$

where, v is the drift velocity of a dispersed particle (m/s) and E is the applied electric field strength. The ζ-potential (mV) was calculated via the Smoluchowski Equation 14:

$$\mu = \frac{\xi \varepsilon}{\eta} \quad (14)$$

which is valid for $r >> \kappa^{-1}$, where ε is the electric permittivity of the solvent, η is the solvent viscosity (Pa s), r is the radius of particle and κ^{-1} is the Debye length. Each individual ζ-potential data point shown was calculated from the average and standard deviation of at least five readings made on the triplicate samples.

2.2.7 Confocal scanning laser microscopy (CLSM)

The microstructure of the WPM- and HT WPM-stabilized emulsions before and after *in vitro* gastric and intestinal digestion was studied using a Zeiss LSM 700 confocal microscope (Carl Zeiss MicroImaging GmbH, Jena, Germany). Nile Red (1 mg mL^{-1} in dimethyl sulfoxide, 1:100, v/v) was used to stain oil (argon laser with an excitation line at 488 nm) and Fast Green (1 mg mL^{-1} in Milli-Q water, 1:100, v/v) was used to stain protein (He-Ne laser with an excitation line at 633 nm). A small quantity of emulsions before and after digestion was placed on a concave confocal microscope slide immediately after *in vitro* digestion, mixed with 10 μL of Nile Red (0.1% w/v) and 12 μL of Fast Green, stained for 15 min. Xanthan gum (50 μL, 0.5% w/v in Milli-Q water water) was used to fix the sample (50 μL) on the slide, covered with a cover slip and finally imaged using a 63× magnification oil immersion objective lens.

2.2.8 Analysis of peptic hydrolysis of interfacial protein

The protein composition at the interface of the emulsion droplets after gastric hydrolysis by pepsin was determined by analysing the cream phase using sodium dodecyl sulphate polyacrylamide gel electrophoresis (SDS-PAGE) under reducing conditions [37]. The emulsion-SGF mixtures (2 mL) after digestion at different times were mixed with 0.5 mL of 0.2 M Na_2CO_3 at pH 7.0 to stop digestion, centrifuged for 20 min at 4200 *g* at 20 °C. The cream layer was carefully removed, dispersed in Milli-Q water and again centrifuged at for 20 min at 4200 *g* at 20 °C. The cream layer was collected carefully and a certain amount of cream was spread on to a filter paper (Whatman No. 42, Whatman International Ltd., Maidstone, Kent, UK) and dried. The dried cream was then mixed with SDS buffer (0.5 M Tris, 2.0% SDS, 0.05% β-mercaptoethanol, pH 6.8), sample:sample buffer = 50 μg:150 μL, and heated to 95–100 °C for 5 min. SDS-PAGE was carried out by loading 10 μL of sample on to gels previously prepared on a Mini-PROTEAN II system (Bio-Rad Laboratories, Richmond, CA, USA). The resolving gel contained 16.0% acrylamide and the stacking gel was made up of 4.0% acrylamide. After running, the gel was stained for 45 min with a Coomassie Brilliant Blue R-250 solution in 20% isopropanol. The gels were destained with a solution of 10% acetic acid and 10% isopropanol and scanned using a Gel Doc™ XR+ System (Bio-Rad Laboratories, Richmond, CA, USA). The intensities of the protein bands were quantified using Image Lab Software Version 5.2.1. The percentage composition of each sample was determined by scanning the gradual reduction in peak volume intensity for each intact protein bands of WPI (Beta Lactoglobulin (β-Lg), β-Lg dimer, Alpha lactoglobulin (α-La), Bovine serum albumin (BSA), as a function of digestion time.

2.2.9 Statistical analysis

All experiments were carried out in triplicate using freshly prepared samples. The results were then reported as mean and standard deviations of these measurements. The statistical analyses were carried out using analysis of variance (ANOVA) using SPSS software (IBM SPSS Statistics for Windows, Version 22.0. Armonk, NY: IBM Corp) and differences were considered significant when $p < 0.05$ were obtained.

3. Results and discussion

3.1 Characterization of WPM particles

As shown in **Figure 1**, the particle size distribution of the 1.0 wt% WPM particles in phosphate buffer at pH 7 was bimodal with a significant proportion of particles in the peaks of 0.1 and 10 μm. The CLSM image (**Figure 1**B) shows the WPM particles stained by Fast Green dye as green spherical shaped particles showing higher fluorescence brightness than the background whey protein gel. The TEM image (**Figure 1**C) shows spherical WPM particles with a diameter of 250-300 nm

in a spatially continuous protein matrix, formed by the aggregation of globular whey proteins on heat treatment [38]. The heat treatment at 90 °C promoted the conversion of the parent whey proteins into covalently cross-linked gel via intramolecular disulfide bonds [32]. The size reduction of the gel owing to the homogenization led to the formation of microgel particles characterized by Sauter mean diameter (d_{32}) of ~ 0.3 µm (**Table 1**).

As expected, the volume mean diameter (d_{43}) was significantly higher (~ 17 µm) due to the presence of aggregates of particles as evidenced by the cloudy appearance of the visual image (**Figure 1**A). It seems that the microgel particles might not have been fully de-aggregated during the two-stage homogenization or might have re-clustered. To avoid dominance of scattering by these large clusters in the Zetasizer cell, the WPM aqueous dispersion was centrifuged at 3000 rpm for 20 min to separate out these aggregates before carrying out dynamic light scattering.

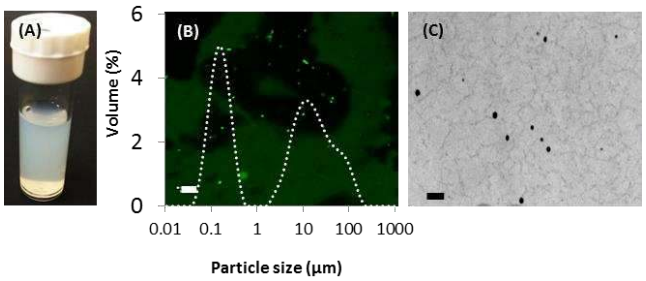

Figure 1. Micrographs at various length scales and superimposed particle size distribution 1 wt% WPM particles in phosphate buffer at pH 7.0. (A) Macroscopic image (B) CLSM, bright green dots representing the WPM particles in protein matrix stained using Fast Green, and black colour represents air or water, scale bar is 5 µm and (C) TEM, black dots representing the WPM particles, scale bar is 500 nm.

Table 1. Mean particle size and zeta potential of WPM particles

	d_{32} (µm)	d_{43} (µm)	Z-average diameter (nm) in supernatant	ζ-potential (mV)
Whey protein microgel particles (WPM)	0.29± 0.02	16.70± 0.19	311± 26	-36.5± 1.5

The Z-average diameter of 311 nm (**Table 1**) with a low polydispersity index (0.15) was in good agreement with d_{32} value and the particle size observed in the micrographs. The Z-average diameter and ζ-potential of the WPM particles at pH 7.0 was in good agreement with a previous study [28], where these soft particles were obtained by a different processing route.

3.2 Characteristics of emulsions stabilized by WPM particles before and after heat treatment

It can be observed from **Figure 2** that the droplet size distribution of WPM-stabilized emulsion was bimodal with a significantly larger proportion of droplets in peak area of 10-100 µm. The peak area with particle size of 0.1-1 µm mostly likely corresponds to the free microgel particles rather than emulsion droplets. Interestingly, HT WPM-stabilized emulsions had a very similar trend with no significant changes in the width of the distribution on thermal treatment. Good stability of both WPM and HT WPM-stabilised emulsions were further evidenced by the absence of free oil and no visible coalescence upon subsequent storage for 6 months. **Table 2** shows the droplet characteristics of the WPM- and HT WPM-stabilized emulsions. Since the emulsion droplets were stabilized by WPM particles of nearly 0.3 µm mean diameter, the relatively larger size of the emulsion droplets (d_{43} = 43 µm), compared to that obtained by a typical molecular surfactant or protein, is expected. The size ratio of WPM particle-to-droplet is 0.006, which is within the typical size ratio for Pickering stabilised emulsions [12].

The ζ-potentials of both sets of emulsion droplets were slightly higher in magnitude (-42 mV) as compared to that of the microgel particles themselves (-36.5 mV) at pH 7.0, which suggests a high concentration of WPM particles at the droplet surfaces.

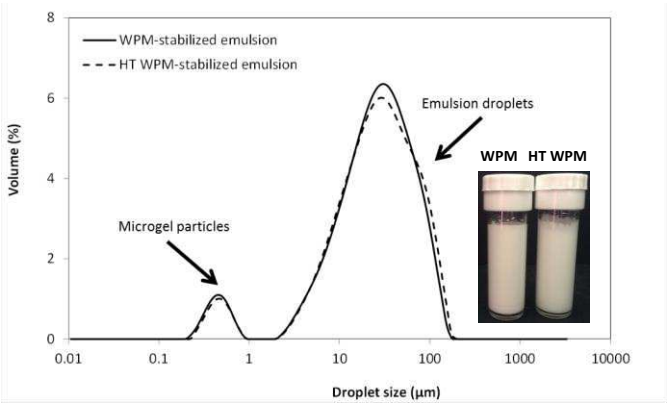

Figure 2. Droplet size distribution of the 20% O/W WPM-stabilized (solid line) and HT WPM-stabilized (dashed line) pickering emulsions. Inset shows macroscopic images of the emulsions.

The mean particle diameters (d_{32}, d_{43}) (**Table 2**) of WPM and HT WPM showed no differences *(p>0.05)*. This suggests that heat treatment at 90 °C did not cause any droplet flocculation or coalescence [31, 39].

Table 2. Mean droplet size, adsorption efficiency, surface coverage and ζ-potential of 20 % O/W emulsions stabilized by whey protein microgels before and after heat treatment.

Emulsions	d_{32} (µm)	d_{43} (µm)	Adsorption efficiency (%)	Surface protein coverage (mg/ m^2)	ζ-potential (mV)
WPM-stabilized emulsions	5.69± 0.39	42.9± 1.26	33± 1.5	14.06± 0.56	-42.3± 0.5
HT WPM-stabilized emulsions	6.02± 0.52	42.8± 2.13	55± 2	23.59± 0.18	-40.5± 0.7

Interestingly, the adsorption efficiency of the particles and consequently the surface coverage increased significantly on heat treatment *(p>0.05)*. Heat treatment of emulsion stabilized by whey

proteins are known to cause inter-droplet interactions when heated at 65-80 °C as they are only partially unfolded, which increases surface hydrophobicity of the interfacial whey protein [31]. However, at higher temperatures (90 °C, as in our case), whey proteins become fully unfolded and are able to rearrange effectively all non-polar amino acids towards the oil phase, thus reducing the tendency for aggregation. Hence, it might be a possibility that the heat treatment promoted WPM particle-particle fusion on the surface of the droplets rather than inter-droplet interactions as reported in previous literatures [31, 39, 40].

The TEM images (**Figure 3A1** and **Figure 3A2**) show clearly that WPM particles were adsorbed on the surface of the emulsion droplets. However, the surface coverage by clearly distinguishable WPM particles seems to be rather incomplete. The WPM particles appeared aggregated, with most of these clusters closely associated with droplet surfaces. It is well known that coverage by distinct surface active particles does not need to be complete to produce stable Pickering emulsions, as long as the adsorbed particle layer forms a rigid network [24, 41, 42]. In the case of the HT WPM emulsions (**Figure 3B1** and **Figure 3B2**), the interface was covered mostly by a continuous network of fused or aggregated particles rather than individual discernible WPM particles. It seems that heat treatment affected individual particle integrity at the interface to a certain extent without influencing the droplet size. Interestingly, in HT WPM-stabilized emulsions, the layer of particles **(Figure 3B1** and **Figure 3B2)** appeared to be shared between neighbouring emulsion droplets [43] and appeared more densely packed as compared to that of non-heated samples, in agreement with the higher surface coverage found in latter case. Thus, particle stabilization of the emulsions is maintained on heat treatment and better coverage is obtained [44].

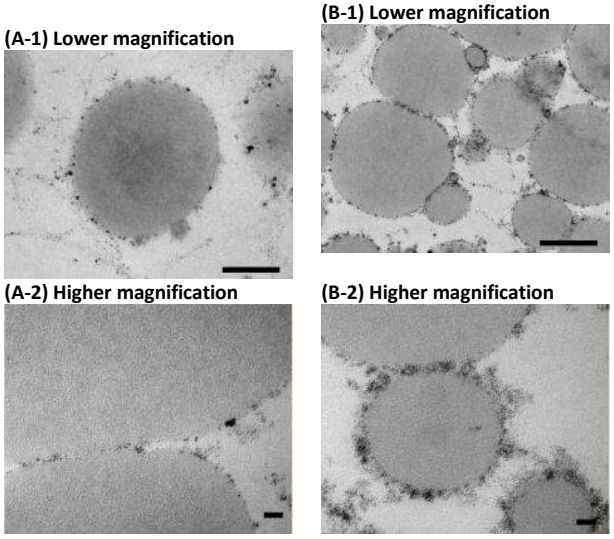

Figure 3. TEM micrographs of 20% o/w emulsions stabilized by whey protein microgel before (A) and after heat treatment (B). Scale bars in (i) and (ii) represent 20 μm and 20 nm, respectively.

3.3 *In vitro* gastric digestion

Figure 4 shows the evolution of droplet size and ζ-potential as a function of *in vitro* digestion time. Interestingly, there was a slight decrease in d_{43} value within the first 10 minutes followed by a steady plateau for both the emulsions. The stability of emulsion droplet size in SGF even after 120 minutes of gastric digestion of WPM and HT WPM emulsions is strikingly different compared to that of typical whey protein-stabilized emulsions. The latter typically shows a dramatic increase in the droplet size due to pepsin-induced rupture of the interfacial protein layer, followed by flocculation and coalescence[14, 37]. Two hypotheses can be proposed for such distinct behaviour of our particle-stabilized emulsions. Pepsin might be unable to access the hydrophobic sites due to potential reburial of those domains within the microgel particles. Alternatively, one might argue that the pepsin was able to access the hydrophobic sites exposed to the continuous phase but the proteolytic activity was not sufficient to digest all the WPM particles or fused HT WPM particles at the interface. Interestingly, both emulsions had sufficient positive surface charge (+40 mV) at pH 2 on addition of SGF, even after 120 minutes of gastric digestion, which further supports the presence of microgel particles rather than just peptides at the interface [37].

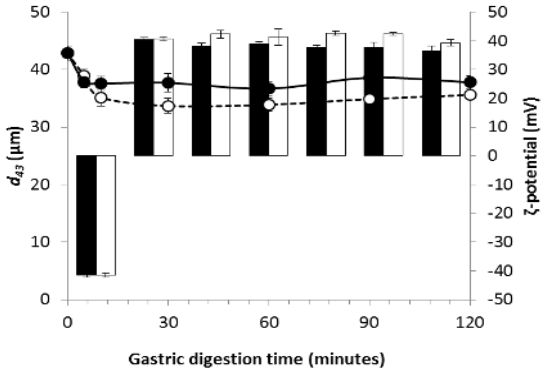

Figure 4. Droplet size (represented as circles) and zeta potential (represented as bars) of 20% o/w emulsions stabilized by whey protein microgel before and after heat treatment. Black represents WPM- and white represents HT WPM-stabilized emulsions . Error bars represent the standard deviation.

The microstructures of the gastric-digested emulsions obtained via CLSM at different times are shown in **Figure 5**. Before addition of pepsin, the HT WPM-stabilized emulsions (**Figure 5B1**) again showed more fused layers of particles as compared to individual WPM particles in the case of the non-heat-treated emulsions (**Figure 5A1**). In comparison to TEM micrographs (**Figure 3**), the microgel particles at the interface appear to have a more swollen and "fluffy morphology" in the CLSM images. This might be attributed to the dehydration step used in TEM micrograph preparation, which results in some degree of shrinkage of these swollen microgel particles, despite fixation by glutaraldehyde and OsO4 [45]. However, it appears that pepsin digested the aggregated protein network, which potentially formed bridges between particles (**Figure 5A2**), consistent with the initial decrease of d_{43} values. Careful observation of the droplets in the micrograph reveals that the droplets were covered by fragments of particles at 120 minutes (**Figure 5A3**), rather than intact discernible particles. In case of the HT WPM emulsions, the interfacial layer appeared thinner compared to the parent emulsion. In both the WPM and HT WPM emulsion, no coalesced droplets were observed. This is unlike the behaviour of typical whey protein-stabilized emulsions which

shows detectable amount of oiling off during gastric digestion, possibly due to the inability of fragmented peptides generated to protect the oil droplets against droplet coalescence [37]. Thus both WPM particles and HT WPM fused particles offered a good protection to oil droplets against coalescence during gastric digestion as compared to typical protein-stabilized interfaces [40].

Figure 6 describes the interfacial composition of the gastric digested interfaces, in terms of bovine serum albumin (BSA) (66 kDa), *α*-Lactalbumin (*α*-La) (14 kDa), *β*-Lactoglobulin dimers (*β*-Lg dimers) (36 kDa), *β*-lactoglobulin monomers (*β*-lg) (18 kDa) as determined by SDS-PAGE.

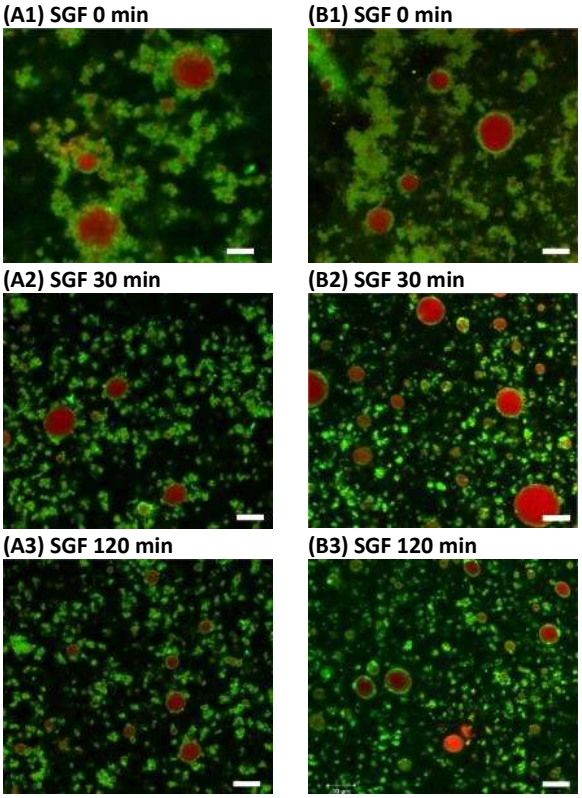

Figure 5. Microstructure of 20% o/w emulsions stabilized by whey protein microgel (A) and after heat treatment (B) as a function of gastric digestion time at pH 2. Green colour represents protein (stained by Fast green) red colour represents the oil phase (stained by Nile Red), and black colour represents air or water. Scale bar represents 10 µm.

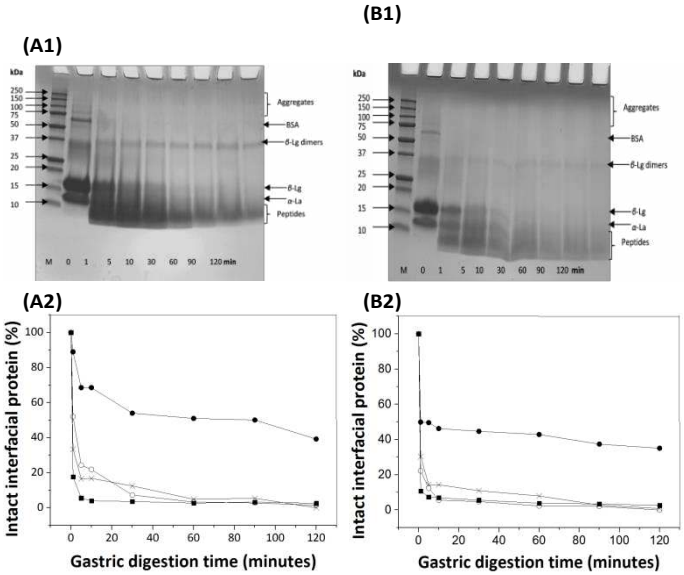

Figure 6. Reduced SDS-PAGE patterns (i) and quantification of intact protein bands (ii) obtained from adsorbed phase of whey protein microgel-stablized emulsions during gastric digestion with added pepsin: A, non-heated; B, heat treated. Symbols represent intact *β*-Lg monomer (○),*β*-Lg dimer (●), BSA (■) and *α*-La (×) at the interface as a function of gastric digestion time.

It can be clearly observed that BSA band disappeared rapidly during just a few minutes of proteolysis, in both WPM- and HT-WPM treated interfaces. The kinetics of pepsin digestion of *α*-La and *β*-Lg were slower in the WPM- as compared to the HT WPM interfaces during first 10 minutes followed by rapid digestion in both systems. The whey proteins were gradually hydrolysed into peptides <10 kDa as the digestion proceeded. Interestingly, there was a significant proportion of *β*-lg dimers (40% and 35% in case of WPM and HT WPM interface, respectively), which were still intact in both the systems even after 2 hours of digestion. Hence, the thin interfacial layer observed in the CLSM micrographs might be a combination of *β*-lg dimers and high molecular weight peptides.

3.4 *In vitro* intestinal digestion and free fatty acid release kinetics

At the start of *in vitro* intestinal digestion, the gastric digested WPM- and HT WPM-stabilized emulsions were exposed to neutral pH (pH 6.8), salts, pancreatin and bile salts. As can be observed in **Figure 7A1** and **Figure 7A2**, both the WPM- and HT-WPM stabilized emulsions showed a steady increase in d_{43} value as time progressed. At 30 min, the droplet size distribution was bimodal with prominent peaks at about 100 and 1000 µm in case of WPM-stabilized emulsions (**Figure 7B1**). The area of the peaks at 100 µm gradually increased as a function of digestion time for both WPM and HT WPM-stabilized emulsions to a maximum at 180 min (**Figure 7B1** and **Figure 7B2**). The substantial increase in d_{43} *value* is consistent with CLSM micrographs showing larger individual coalesced oil droplets (**Figure 8**). It therefore appears that the instability of these emulsions under simulated intestinal digestion is linked to the digestive action of the lipase within the pancreatin. During action of pancreatic lipase, surface-active free fatty acids (FFAs) and mono-acylglycerols (MAG) are expected to be generated

at the droplet surfaces. Coalescence of emulsion droplets can be driven by these surface-active FFAs and MAG, which are comparatively less effective at stabilizing oil-in-water emulsions against coalescence than the gastric-digested microgel particles at the interface [20]. Although the CLSM micrographs still showed significant WPM particles or peptides remaining at the interface in the case of WPM-stabilized emulsions as compared to the HT WPM stabilized interfaces, the adsorbed layers were obviously not sufficiently viscoelastic and coherent to provide sufficient colloidal stability to the droplets.

The kinetics of intestinal digestion of 20 wt% O/W emulsions stabilized using whey protein microgels in the presence of bile salts and pancreatin was followed using a pH-stat method (**Figure 9**). Generally, whey proteins adorbed at oil-water interfaces can easily be displaced by bile salts and thus the oil easily accessed by lipase to generate FFAs and MAG. Even in the case of heat-treated whey protein isolate-stabilized emulsions, bile salts are known to create defects in the protein network at the cross-linked interface and thus access to lipase is established [18, 46]. Both WPI and heat treated WPI-stabilized emulsions generated approximately 46% of FFAs derived from the long-chain FFAs from sunflower oil that tend to accumulate at the oil–water interface and inhibit further lipase activity [21, 36].

However, in case of WPM and HT-WPM stabilized emulsions, the extent of fatty acid release was slightly lower than the WPI emulsions (46%) generating approximately 42% of FFAs. Even the rate of release was slightly lower as compared to that of WPI emulsions as shown in **Figure 9**. Interestingly, there was no significant difference between WPM and HT WPM emulsion in terms of rate and extent of fatty acid release *($p > 0.05$)*. This supports the particle size and microstructural results that suggested that both the emulsion types were prone to lipolysis. Both emulsions had similar concentrations and type of peptides and remnants of *β*-lg dimers after gastric digestion. Half times of 6.6 min were observed for microgel-stabilized emulsions which is twice that required for digestion of normal *β*-lg stabilized interfaces ($t_{1/2}$ = 2.84 mins) [36].

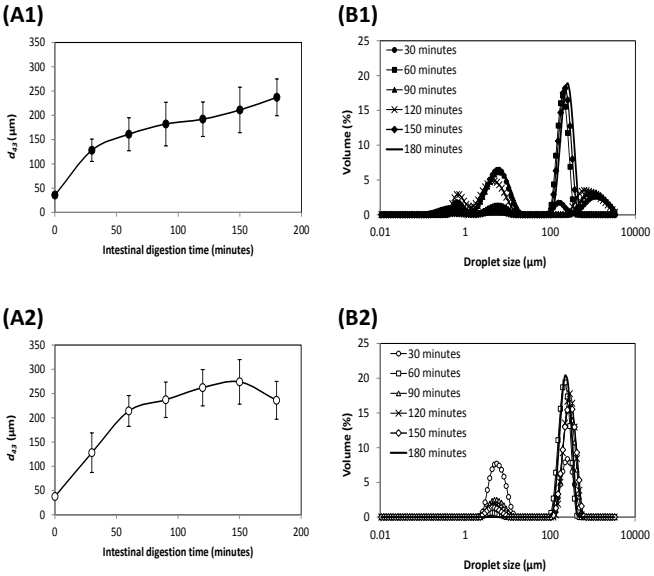

Figure 7. Mean droplet size (A) and distribution (B) of WPM (closed symbols) and HT WPM-stabilized emulsions (open symbols) as a function of time in presence of simulated intestinal fluid (containing bile salts and pancreatin).

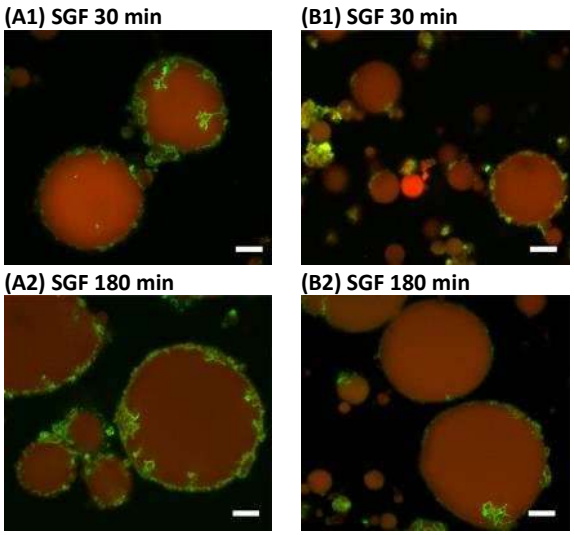

Figure 8. Microstructure of (A) WPM and (B) HT WPM-stabilized emulsions as a function of digestion time. Green colour represents protein (stained by Fast green) red colour represents the oil phase (stained by Nile Red), and black colour represents air or water. Scale bar represents 50 μm.

Nevertheless, this reduction in lipolysis rate is not sufficiently large to support our hypothesis that microgel particles at the interface might be able to significantly delay lipid digestion. This is because gastric digestion will play a key role in the case of a protein-based microgel system as seen in our study. However, a key question is whether proteolysis of the particles at the interface is first required in-order for bile to replace them and lipase to adsorb and release fatty acids.

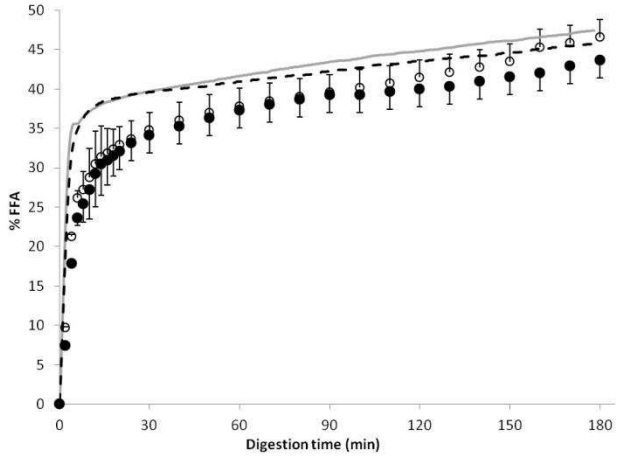

Figure 9. Kinetics of fatty acid release (lipolysis) from 20 wt% O/W emulsions stabilized whey protein microgels (solid circles) with or (open circles) without heat treatment when they are exposed to pancreatin and bile salts, post gastric digestion. Free fatty acid release curves of lipolysis of WPI-stabilized emulsion without (gray solid line) or with (black dashed line) heat treatments are included for comparison. Error bars denote standard deviation of three measurements.

3.5 Influence of bile salts and pure lipase on intact WPM- and HT WPM- interfaces

In order to investigate whether the initially adsorbed WPM particles or a fused HT particle network can be displaced by bile salts directly, simulated intestinal digestion of the WPM and HT-WPM emulsions were conducted. This was done using pure lipase and bile salts without any of the proteolysis that normally occurs during the gastric digestion stage.

Figure 10 shows that the influence of bile salts and SIF buffer was minimal *($p > 0.05$)* on the particle size in case of both WPM and HT-WPM stabilized emulsions. The *ζ*-potential of emuslion droplets changed from -40 mV to -36 mV on addition of the SIF buffer. It is worth noting that the *ζ*-potential of emulsion droplets saturated with pure bile extract is around −54 mV [47] and the WPM and HT-WPM stabilized emulsions reach those magnitudes in presence of bile salts. Some flocculation was observed visually on addition of SIF buffer and buffer containing bile salts, which can be attributed to the increase in electrolytes such as Na^+, K^+, screening the charge of the microgel particles. However, no coalescence of droplets was detected. These results suggest that bile salts cannot directly desorb the particles or the fused particle layer from the interface, contradicting the initial hypothesis. Since, the microgel particles were anionic surface-active agents, they were also likely to retard anionic bile salts from the vicinity of the interface.

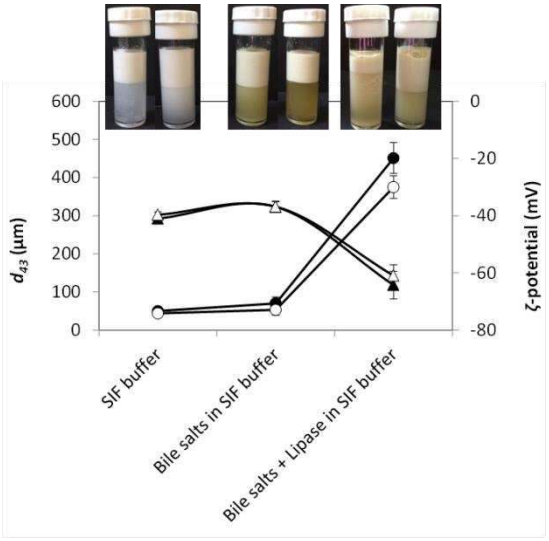

Figure 10. Droplet size (represented by circles), zeta potential (represented as bars) and corresponding visual images of WPM and HT-WPM emulsions on treatment with SIF buffer, bile salts and lipase. Black represents WPM- and white represents HT WPM-stabilized emulsion.

In contrast to this behaviour in presence of bile salts alone, **Figure 10** shows that the droplet size increased significantly to over 350 µm after the digestion with pure lipase in both emulsions. The visual images also showed some oiling off indicating coalescence. The appreciable decrease of *ζ*-potential values *($p < 0.05$)* for both emulsions after digestion with lipase to -60 mV may be attributed to adsorption of lipase with subsequent release of FFA and mono-acylglycerol at the interface. This suggest that lipase itself can access the O/W interface and release fatty acids, even if the interface is not displaced by bile salts.

As it might be expected, for both WPM and HT-WPM stabilized emulsions, the extent of fatty acid release when exposed to just lipase was lower than when exposed to both bile salts and pancreatin generating approximately 20% of FFAs (**Figure 11**) as compared to 42% of FFAs, respectively. It is interesting to note that despite Eq 8 only being established for short times, no large departures from the model are seen here for large times (>120 min). As expected, the fitted release had reaction rate constants similar in value (k = 0.31 and 0.35 mol s^{-1} m^{-2}) suggestive of the fact that the kinetics after the enzyme has got access to the interface are equivalent. The presence of intact particles or a fused layer of particles has no influence on the reaction rate induced by the enzyme (pure lipase) once the latter is adsorbed at the droplet surfaces. Thus, the limiting factor is the rate of enzyme adsorption to the droplet surface, which is of course expected to be difficult for the two cases. However, the overall rate of digestion for the heat-treated emulsion ($t_{1/2}$=44.44 min) was 2.5 times delayed as compared to that of the non-heat-treated case ($t_{1/2}$=16.52 min). An explanation of the difference in overall kinetics and extent of lipolysis of WPM and HT-WPM emulsion is illustrated via the schematic in **Figure 11** and theoretical packing considerations. The bile salts, being small molecules, can probably pass through the gaps in the microgel-stabilized interface and adsorb at the interface, but they cannot easily displace the microgel particles, due to the very strong binding of latter to the interface.

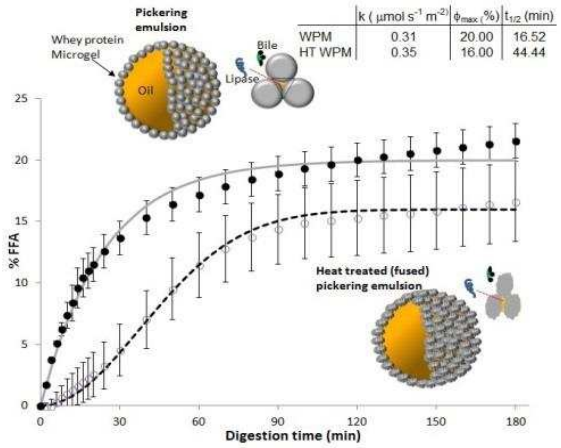

	k (μmol s^{-1} m^{-2})	ϕ_{max} (%)	$t_{1/2}$ (min)
WPM	0.31	20.00	16.52
HT WPM	0.35	16.00	44.44

Figure 11. Kinetics and schematic diagram of proposed mechanism of fatty acid release (lipolysis) from 20 wt% O/W emulsions stabilized by WPM (solid circles) or HT-WPM (open circles) when they are exposed to pure lipase and bile salts. The curves are the best fits to the experimental data predicted using the mathematical model (equation 8) for WPM (gray solid line), (equation 9) for HT-WPM (black dashed line). Equations 8 and 9 respectively model the rapid surface enzyme adsorption case and diffusion inhibited situation, latter arises due to the heat treatment of microgel particles. Error bars denote standard deviation of three measurements.

The inability of bile salts to displace the microgel particles from the interface means that a large portion of the surface is not available for the adsorption of lipase/colipase complex. This will reduce the overall rate of FFA generation, but does not necessarily hide the lipase from getting in contact with the uncovered patches between the particles.

To gain a rough idea of the available surface fraction, let us consider an idealised case of monodispersed spherical particles. For such a system, the highest coverage is achieved when particles on the surface of droplets are placed on a regular 2D triangular lattice. In such an arrangement the number of particles per unit area is $2/(\sqrt{3}d_0^2)$. If the contact angle for the particles on the oil-water interfaces (measured into the denser aqueous phase) is θ, then the area occupied by each microgel particle is $(\pi d_0^2 sin^2\theta)/4$, where $\theta < 90^\circ$ for an oil-in-water Pickering emulsion. Thus, the free remaining surface fraction is $1 - [(\pi sin^2\theta)/(2\sqrt{3})]$, which evaluates to around 9% for a contact angle of 90°. The area fraction is significantly larger at 55%, when θ is 45°. A more disordered arrangement of particles will serve to increase the unoccupied area, while some degree of polydispersity will help to reduce it.

The radius of gyration of the pancreatic lipase/co-lipase complex is approximately 25 Å [48], so this can easily penetrate the microgel particles and gain access to the O/W interface. The typical dimension of gaps between the microgel particles, arranged on the triangular lattice, is $(\sqrt{3}-1)d_0/2 \approx 110$ nm, for particles of size d_0 = 300 nm. This is far larger than the 2.5 nm that is required to have any kind of substantial impact on preventing the diffusion of lipase/colipase complex to the droplet interface. The large estimated gap size, in particular for non-heat treated systems (WPM-stabilized interface) where no real opportunity for decreasing the gaps between particles arises, largely limits the ability of microgel layers to act as effective physical barriers against the incoming enzyme.

In case of the heat-treated fused particle layer (HT-WPM-stabilized interface), the gaps were expected to be significantly smaller, which might have impeded all aspects of the process, including the diffusion of digestion products such as FFA away from the reaction sites, as well as that of lipase/bile salts complex to the surface. This possibly led to the observed as well as predicted delay in the FFA release in the case of the heat treated Pickering emulsion.

4. Conclusions

Findings from our study demonstrate that specific design of O/W Pickering emulsions using food grade WPM particles can have a significant impact on controlling the rate and extent of digestion of the emulsified lipids by lipase, under simulated intestinal conditions without prior gastric step. This is driven by the inability of bile salts to displace the soft deformable WPM particles from the interface, which are effectively irreversibly adsorbed. The kinetics of digestion were further slowed when O/W emulsions stabilized by WPM particles were heat-treated, which resulted in generation of a fused layer of particles, and thus higher surface packing as characterized by interfacial adsorption density measurements, adsorption efficiency and structural visualization (transmission electron microscopy). We have also shown that there is an interesting correlation between surface packing density by microgel particles (regular 2D triangular lattice assumption) and lipid digestibility (as determined by fatty acid release and quantitative estimations of maxima, kinetics and half-life).

When simulating the overall gastrointestinal digestion using an *in vitro* model, our study highlighted that WPM microgels were broken down by proteases irrespective of whether further heat treatment was applied or not during the *in vitro* gastric transit, as evidenced by SDS PAGE, surface charge measurements and confocal microscopy. Such protease-responsive nature of the WPM particles enhanced the lipolysis kinetics of Pickering emulsions significantly, due to the interfacial presence of remnants of particles/ peptides as compared to intact microgel particles during *in vitro* intestinal digestion. These promising results suggest that engineering the interface with biocompatible and biodegradable Pickering stabilizers and tuning them with thermal treatment has implications in rational designing of novel food to combat issues of obesity/weight management and designing pharmaceutical applications with tailored properties such as sustained release of lipophilic molecules for various routes of administration. Future work is underway to understand the kinetics and fine detail of the FFA and monoacyl glycerol release (which is not released into the continuous phase) and its contribution to the self-assembly process in creating nanostructures during lipid digestion using small angle X-ray scattering (SAXS).

Acknowledgements

The authors would like to gratefully acknowledge the contributions of Martin Fuller and Dr. Sally Boxal for their technical support in electron and confocal microscopy imaging at Bio-imaging Facility

within the Faculty of Biological Sciences of the University of Leeds. One of us (RE) wishes to thank Eric Dickinson for useful discussions regarding the kinetics of lipid conversion.

References

1. W. Ramsden, *Proceedings of the Royal Society of London*, 1903, **72**, 156-164.
2. S. U. Pickering, *Journal of the Chemical Society, Transactions*, 1907, **91**, 2001-2021.
3. J. Tang, P. J. Quinlan and K. C. Tam, *Soft Matter*, 2015, **11**, 3512-3529.
4. Y. Chevalier and M.-A. Bolzinger, *Colloids and Surfaces A: Physicochemical and Engineering Aspects*, 2013, **439**, 23-34.
5. E. Dickinson, *Trends in Food Science & Technology*, 2012, **24**, 4-12.
6. E. Dickinson, *Trends in Food Science & Technology*, 2015, **43**, 178-188.
7. C. C. Berton-Carabin and K. Schroën, *Annual Review of Food Science and Technology*, 2015, **6**, 263-297.
8. M. Wahlgren, J. Engblom, M. Sjoo and M. Rayner, *Current Pharmaceutical Biotechnology*, 2013, **14**, 1222-1234.
9. B. P. Binks, *Current Opinion in Colloid & Interface Science*, 2002, **7**, 21-41.
10. R. Aveyard, B. P. Binks and J. H. Clint, *Advances in Colloid and Interface Science*, 2003, **100–102**, 503-546.
11. F. Leal-Calderon and V. Schmitt, *Current Opinion in Colloid & Interface Science*, 2008, **13**, 217-227.
12. R. Ettelaie and S. V. Lishchuk, *Soft Matter*, 2015, **11**, 4251-4265.
13. B.-S. Chu, G. T. Rich, M. J. Ridout, R. M. Faulks, M. S. J. Wickham and P. J. Wilde, *Langmuir*, 2009, **25**, 9352-9360.
14. M. Golding, T. J. Wooster, L. Day, M. Xu, L. Lundin, J. Keogh and P. Clifton, *Soft Matter*, 2011, **7**, 3513-3523.
15. A. Sarkar, J.-M. Juan, E. Kolodziejczyk, S. Acquistapace, L. Donato-Capel and T. J. Wooster, *Journal of Agricultural and Food Chemistry*, 2015, **63**, 8829-8837.
16. H. Singh and A. Sarkar, *Advances in Colloid and Interface Science*, 2011, **165**, 47-57.
17. A. Sarkar, D. S. Horne and H. Singh, *Food Hydrocolloids*, 2010, **24**, 142-151.
18. J. Maldonado-Valderrama, N. C. Woodward, A. P. Gunning, M. J. Ridout, F. A. Husband, A. R. Mackie, V. J. Morris and P. J. Wilde, *Langmuir*, 2008, **24**, 6759-6767.
19. A. Mackie and A. Macierzanka, *Current Opinion in Colloid & Interface Science*, 2010, **15**, 102-108.
20. A. Sarkar, D. S. Horne and H. Singh, *International Dairy Journal*, 2010, **20**, 589-597.
21. M. V. Tzoumaki, T. Moschakis, E. Scholten and C. G. Biliaderis, *Food & Function*, 2013, **4**, 121-129.
22. M. Visanko, H. Liimatainen, J. A. Sirviö, J. P. Heiskanen, J. Niinimäki and O. Hormi, *Biomacromolecules*, 2014, **15**, 2769-2775.
23. M. V. Tzoumaki, T. Moschakis, V. Kiosseoglou and C. G. Biliaderis, *Food Hydrocolloids*, 2011, **25**, 1521-1529.
24. A. Yusoff and B. S. Murray, *Food Hydrocolloids*, 2011, **25**, 42-55.
25. F. Liu and C.-H. Tang, *Journal of Agricultural and Food Chemistry*, 2013, **61**, 8888-8898.
26. Z. Luo, B. S. Murray, A. Yusoff, M. R. A. Morgan, M. J. W. Povey and A. J. Day, *Journal of Agricultural and Food Chemistry*, 2011, **59**, 2636-2645.
27. A. Ye, X. Zhu and H. Singh, *Langmuir*, 2013, **29**, 14403-14410.
28. M. Destribats, M. Rouvet, C. Gehin-Delval, C. Schmitt and B. P. Binks, *Soft Matter*, 2014, **10**, 6941-6954.
29. B. S. Murray and N. Phisarnchananan, *Food Hydrocolloids*, In Press.
30. R. W. Style, L. Isa and E. R. Dufresne, *Soft Matter*, 2015.
31. F. J. Monahan, D. J. McClements and J. B. German, *Journal of Food Science*, 1996, **61**, 504-509.
32. C. Schmitt, C. Moitzi, C. Bovay, M. Rouvet, L. Bovetto, L. Donato, M. E. Leser, P. Schurtenberger and A. Stradner, *Soft Matter*, 2010, **6**, 4876-4884.
33. I. Papageorgiou, T. Abberton, M. Fuller, J. Tipper, J. Fisher and E. Ingham, *Nanomaterials*, 2014, **4**, 485.
34. A. Sarkar, K. K. T. Goh and H. Singh, *Food Hydrocolloids*, 2009, **23**, 1270-1278.
35. M. Minekus, M. Alminger, P. Alvito, S. Ballance, T. Bohn, C. Bourlieu, F. Carriere, R. Boutrou, M. Corredig, D. Dupont, C. Dufour, L. Egger, M. Golding, S. Karakaya, B. Kirkhus, S. Le Feunteun, U. Lesmes, A. Macierzanka, A. Mackie, S. Marze, D. J. McClements, O. Menard, I. Recio, C. N. Santos, R. P. Singh, G. E. Vegarud, M. S. J. Wickham, W. Weitschies and A. Brodkorb, *Food & Function*, 2014, **5**, 1113-1124.
36. Y. Li and D. J. McClements, *Journal of Agricultural and Food Chemistry*, 2010, **58**, 8085-8092.
37. A. Sarkar, K. K. T. Goh, R. P. Singh and H. Singh, *Food Hydrocolloids*, 2009, **23**, 1563-1569.
38. T. Nicolai, M. Britten and C. Schmitt, *Food Hydrocolloids*, 2011, **25**, 1945-1962.
39. A. Sarkar, J. Arfsten, P.-A. Golay, S. Acquistapace and E. Heinrich, *Food Hydrocolloids*, 2016, **52**, 857-867.
40. S. Roth, B. S. Murray and E. Dickinson, *Journal of Agricultural and Food Chemistry*, 2000, **48**, 1491-1497.
41. T. S. Horozov and B. P. Binks, *Angewandte Chemie International Edition*, 2006, **45**, 773-776.
42. R. Ettelaie and B. Murray, *The Journal of Chemical Physics*, 2014, **140**, 204713.
43. D. J. French, P. Taylor, J. Fowler and P. S. Clegg, *Journal of Colloid and Interface Science*, 2015, **441**, 30-38.
44. A. Marefati, M. Rayner, A. Timgren, P. Dejmek and M. Sjöö, *Colloids and Surfaces A: Physicochemical and Engineering Aspects*, 2013, **436**, 512-520.
45. M. Liboff, H. D. Goff, Z. Haque, W. K. Jordan and J. E. Kinsella, *Food Structure*, 1998, **7**, 67-74.
46. L. A. Pugnaloni, E. Dickinson, R. Ettelaie, A. R. Mackie and P. J. Wilde, *Advances in Colloid and Interface Science*, 2004, **107**, 27-49.
47. S. Mun, E. A. Decker and D. J. McClements, *Food Research International*, 2007, **40**, 770-781.
48. D. Pignol, L. Ayvazian, B. Kerfelec, P. Timmins, I. Crenon, J. Hermoso, J. C. Fontecilla-Camps and C. Chapus, *Journal of Biological Chemistry*, 2000, **275**, 4220-4224.